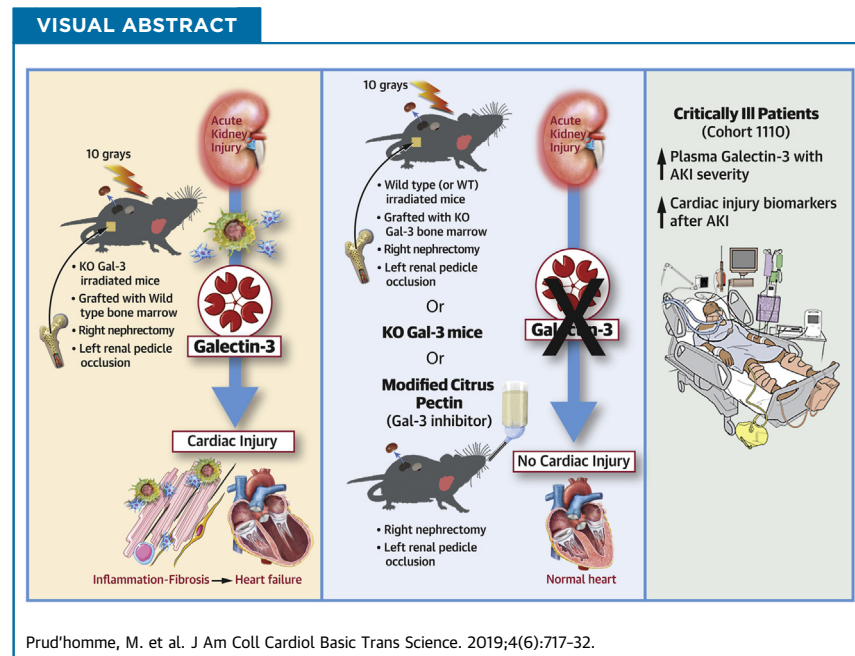


PRECLINICAL RESEARCH

Acute Kidney Injury Induces Remote Cardiac Damage and Dysfunction Through the Galectin-3 Pathway



Mathilde Prud'homme, PhD,^a Maxime Coutrot, MD, MSc,^{a,b,*} Thibault Michel, MD, MSc,^{a,*} Louis Boutin, MD, MSc,^{a,b,*} Magali Genest, PhD,^{a,d} Françoise Poirier, PhD,^c Jean-Marie Launay, PHARM.D, PhD,^a Bocar Kane,^f Satoshi Kinugasa, MD, PhD,^d Niki Prakoura, PhD,^d Sophie Vandermeersch,^d Alain Cohen-Solal, MD, PhD,^{a,e} Claude Delcayre, PhD,^a Jane-Lise Samuel, MD, PhD,^a Ravindra Mehta, MD,^g Etienne Gayat, MD, PhD,^{a,b} Alexandre Mebazaa, MD, PhD,^{a,b} Christos E. Chadjichristos, PhD,^{d,†} Matthieu Legrand, MD, PhD^{a,b,h,†}



HIGHLIGHTS

- In 2 different mouse models, AKI increased Gal-3 expression and induced cardiac dysfunction, cardiac and systemic inflammation, cardiac macrophage infiltration, and fibrosis.
- Cardiac consequences of AKI were dependent on the Gal-3 pathway and were prevented using Gal-3 knockout mice or modified citrus pectin as a pharmaceutical inhibitor.
- Cardiac Gal-3 expression resulted from bone marrow-derived immune cells recruitment after AKI.
- In critically ill patients, development of AKI is associated with increased plasma Gal-3 levels and increased biomarkers of cardiac injury and damage.

From the ^aINSERM UMR-S 942, Institut National de la Santé et de la Recherche Médicale (INSERM), Lariboisière Hospital, and INI-CRCT-F-CRIN, Paris, France; ^bAP-HP, St-Louis-Lariboisière Hospital, Department of Anesthesiology and Critical Care and Burn Unit, University Paris Diderot, Paris, France; ^cInstitut Jacques Monod, Team: Morphogenesis, Homeostasis and Pathologies, Paris, France; ^dINSERM UMR-S 1155, Tenon Hospital, Paris, France; ^eCardiology Department, Lariboisière Hospital, Paris, France; ^fUMS-28 Phénotypage du petit animal, Université Pierre et Marie Curie, Paris, France; ^gDepartment of Medicine, University of California-San Diego, San Diego, California; and the ^hDepartment of Anesthesiology and peri-operative Care, University of California San Francisco, United States. *Drs. Coutrot, Michel, and Boutin contributed equally to this work and are joint first authors. †Drs. Chadjichristos and Legrand contributed equally to this work and are joint senior authors. This work was supported by "Institut

**ABBREVIATIONS
AND ACRONYMS**

AKI = acute kidney injury
BM = bone marrow
BUN = blood urea nitrogen
Cr = creatinine
eGFR = estimated glomerular filtration rate
Gal-3 = galectin-3
KO = knock-out
ICAM = intercellular adhesion molecule
ICU = intensive care unit
IL = interleukin
IR = ischemia-reperfusion
KDIGO = Kidney Disease Improving Global Outcome
MCP = modified citrus pectin
NT-proBNP = N-terminal-pro-brain natriuretic peptide
TGF = transforming growth factor
TNF = tumor necrosis factor
UO = unilateral ureteral obstruction
WT = wild type

SUMMARY

Acute kidney injury is associated with increased risk of heart failure and mortality. This study demonstrates that acute kidney injury induces remote cardiac dysfunction, damage, injury, and fibrosis via a galectin-3 (Gal-3) dependent pathway. Gal-3 originates from bone marrow-derived immune cells. Cardiac damage could be prevented by blocking this pathway. (J Am Coll Cardiol Basic Trans Science 2019;4:717–32) © 2019 The Authors. Published by Elsevier on behalf of the American College of Cardiology Foundation. This is an open access article under the CC BY-NC-ND license (<http://creativecommons.org/licenses/by-nc-nd/4.0/>).

Acute kidney injury (AKI) has been associated with an increased risk of mortality (1), even in patients free of previous cardiovascular comorbidities (2). Furthermore, AKI has been associated with long-term cardiovascular events (3). Whether the occurrence of AKI only reflects the severity and magnitude of underlying disease or may contribute to remote organ injury remains uncertain. Remote cardiovascular injury may contribute to poor outcomes after AKI (4). AKI has also been associated with long-term cardiovascular events. This has been described in type 3 cardiorenal syndrome (or acute reno-cardiac syndrome) (5).

can activate Gal-3–dependent pathways and promote cardiac injury. For this purpose, we explored the role of Gal-3 in cardiac injury after kidney injury. Moreover, a bone marrow (BM) graft from Gal-3 knock-out (KO) mice was used to determine the origin of Gal-3.

METHODS

ANIMALS. Two- to 4-month old male C57Bl6/J mice (Janvier laboratory, Le Genest-Saint-Isle, France) and C57Bl6/J KO mice for Galectin-3 [Gal-3 KO (13)] were used. All animals were randomized into different groups after baseline echocardiography. Methods of echocardiography, plasma assays, gene expression analysis, protein analysis, immunostaining, cardiac fibrosis evaluation, renal macrophage isolation, cell culture, and monocyte adhesion assays are detailed in the [Supplemental Appendix](#).

Renal and hind limb ischemia-reperfusion injury. A right nephrectomy and left renal pedicle occlusion (25 min of ischemia), followed by reperfusion, were performed under anesthesia (intraperitoneal injection of ketamine: 100 mg/kg and xylazine: 20 mg/kg). Right kidneys were used as controls. Sham mice underwent the same procedure, except for renal pedicle occlusion and right nephrectomy (14). To understand the kinetics of the kidney–heart crosstalk after renal ischemia–reperfusion (IR), mice were killed at different time points after reperfusion (at 3, 6, 12, 24, 48, and 72 h, and at 28 days; n = 7 per group)

SEE PAGE 733

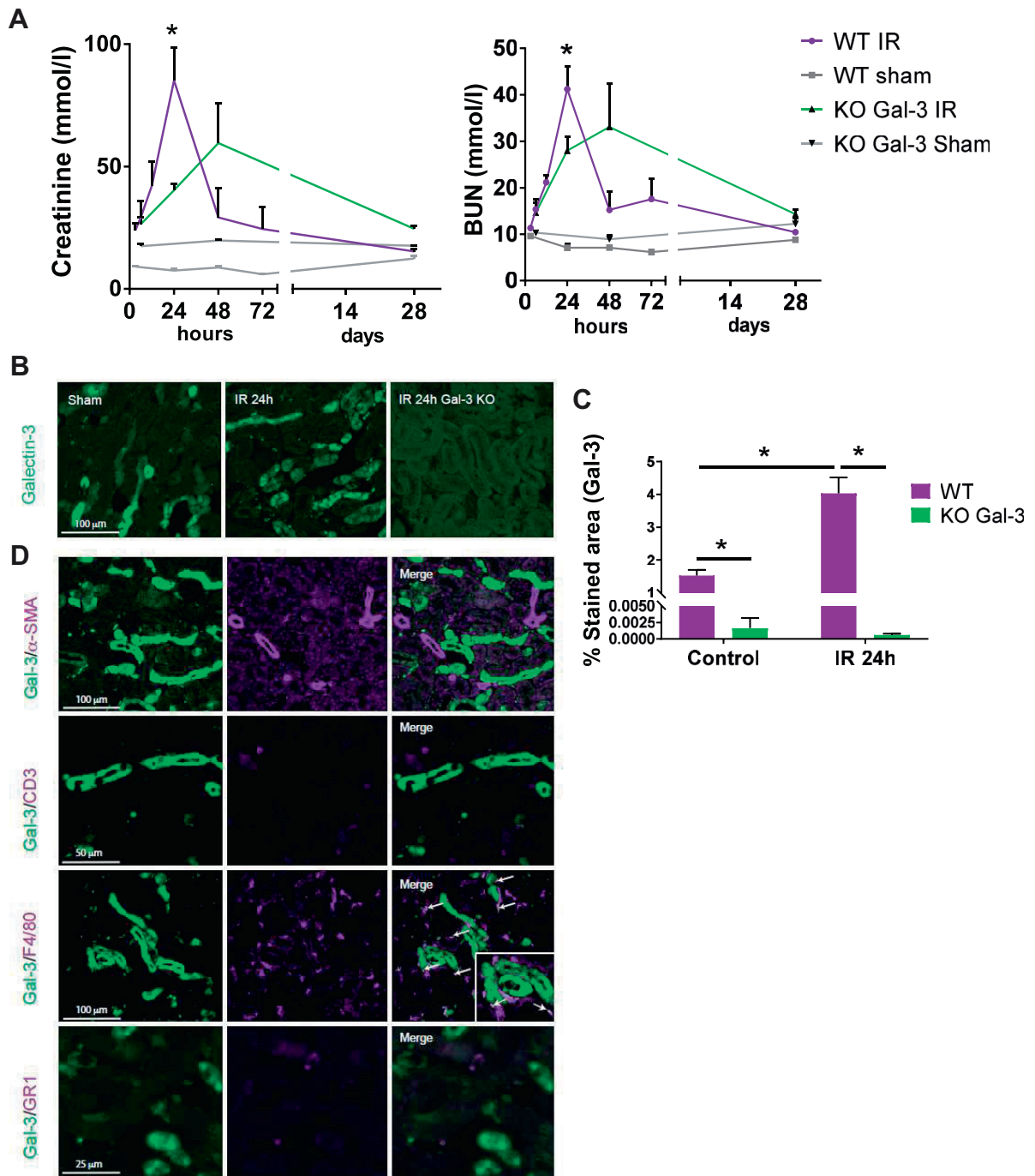
However, whether transient AKI can induce long-term cardiac injury remains unexplored. Cardiac fibrosis has been described as a key feature of chronic heart diseases (6). Galectin-3 (Gal-3) is a lectin that specifically binds to β -galactosides (7) expressed in many tissues, including the heart and kidney (8,9). In the heart, Gal-3 induction promotes myocardial fibrosis and heart failure progression (10,11). Gal-3 has been shown to be a key player in cardiac fibrosis induction and has been proposed as a prognostic biomarker for chronic heart failure (7). In the kidney, Gal-3 has also been shown to be upregulated after AKI (12). In the present study, we hypothesized that AKI

National de la Santé et de la Recherche Médicale (INSERM)” and by Paris Diderot University and the Société Française d’Anesthésie et de Réanimation (SFAR). Dr. Prud’homme was supported by a Ph.D. training grant from Paris Diderot University and “Groupe de Réflexion sur la Recherche Cardiovasculaire (GRRC).” Dr. Cohen-Solal has received grants and fees from Novartis, Servier, Vifor, AstraZeneca, and Merck & Co. Inc. Dr. Mehta has been a consultant, a member of the advisory board for Baxter, AM Pharma, CSL-Behring, Astute Medical Inc. Regulus, Akebia, Intercept, Mallinckrodt, and Ferring; and has received grants from Relypsa, Fresenius-Kabi, Fresenius, and Grifols. Dr. Gayat has been a consultant for Magnisense and Adrenomed; and has received research grants from Deltex Medical and Retia Medical. Dr. Legrand has received research support from Sphingotec; has received lecture fees from Baxter and Fresenius; and has received consultancy fees from Novartis. All other authors have reported that they have no relationships relevant to the contents of this paper to disclose.

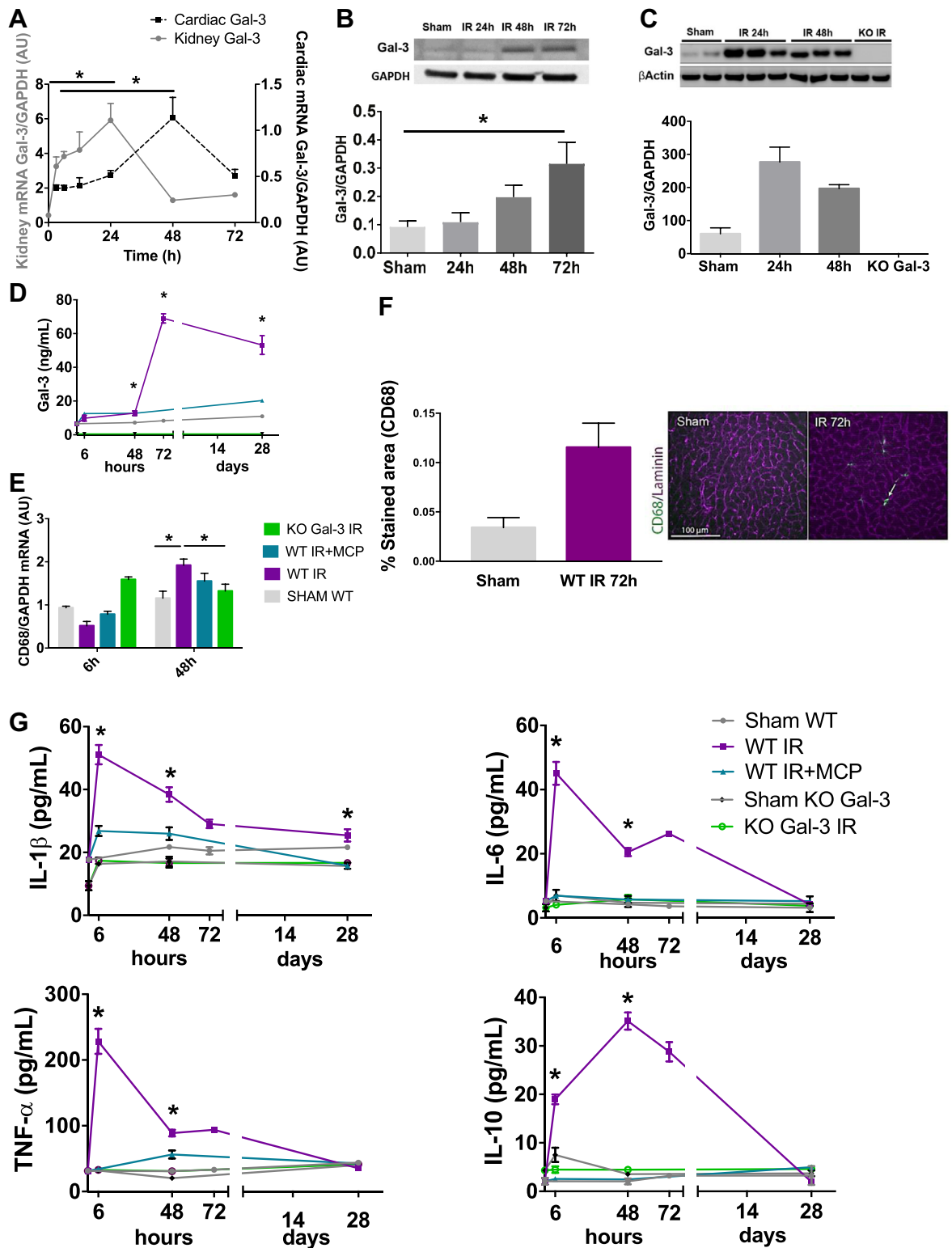
The authors attest they are in compliance with human studies committees and animal welfare regulations of the authors’ institutions and Food and Drug Administration guidelines, including patient consent where appropriate. For more information, visit the *JACC: Basic to Translational Science* [author instructions page](#).

Manuscript received February 21, 2019; revised manuscript received May 29, 2019, accepted June 4, 2019.

FIGURE 1 Renal IR Leads to Acute and Transient Renal Dysfunction With Increased Gal-3 Expression



(A) Plasma assays performed in sham and ischemia–reperfusion IR mice showed an early and transient increase in creatinine and blood urea nitrogen (BUN) levels after IR compared with sham mice ($p < 0.001$; wild-type [WT] IR mice vs. WT sham mice). **(B)** Immunostaining showed increased galectin-3 (Gal-3) expression in kidney tissue, mainly in tubular cells, in response to renal IR. **(C)** Quantification of Gal-3 immunostaining of sham, IR 24-h WT, IR 2-h knockout (KO) Gal-3 groups. After IR, Gal-3 expression is increased in WT mice. **(D)** Gal-3 co-immunostaining with α -smooth muscle actin (SMA) (a marker of smooth muscle cells/myofibroblasts), CD3 (lymphocyte marker), F4/80 (macrophage marker), and GR1 (neutrophil marker) only showed co-localization of Gal-3 with F4/80, indicating that it was also expressed by infiltrated macrophages within the injured renal tissue after 24 h of IR (white arrows). $n = 7$ to 14 for WT IR groups; $n = 4$ to 7 for KO IR; $n = 4$ for WT and $n = 4$ KO Gal-3 sham mice. Data are presented as mean \pm SEM, and comparisons of medians were made using nonparametric Mann-Whitney U test. * $p < 0.05$.

FIGURE 2 Cardiac Inflammation After Renal IR

(Supplemental Figure 1A). Another mouse group was submitted to left femoral artery occlusion for 25 min, followed by reperfusion. These mice were killed 28 days after surgery (hind limb ischemia).

Bone marrow transplantation. Mice were irradiated at 10 grays (2 × 5 grays at 5-h interval) with filter, with a Faxitron irradiator (Faxitron, Tuscon, Arizona). After the second irradiation, mice were grafted with BM from wild-type (WT) or KO mice. At the end of the protocol, 2 groups of chimeric mice were obtained: WT mice grafted with KO Gal-3 bone marrow (WT^{KO BM}) and KO Gal-3 mice grafted with WT bone marrow (KO^{WT BM}). These chimeric mice were submitted to right nephrectomy and left renal IR injury, as described previously. Sham mice underwent the same procedure, except for right nephrectomy and left renal IR (Supplemental Figures 1B and 2).

Unilateral ureteral obstruction. A left ureteral obstruction was performed under anesthesia. The ureter was subsequently ligated in 2 places near the kidney. Sham mice underwent the same procedure, except for ureteral obstruction (Supplemental Figure 1C).

TREATMENTS. The Gal-3 inhibitor modified citrus pectin (MCP) was dissolved in drinking water (100 mg/kg/day). Mice were either pre-treated with MCP (IR+MCP) 3 days before surgery and during the time of reperfusion or treated 1 day after surgery (IR+MCP d+1).

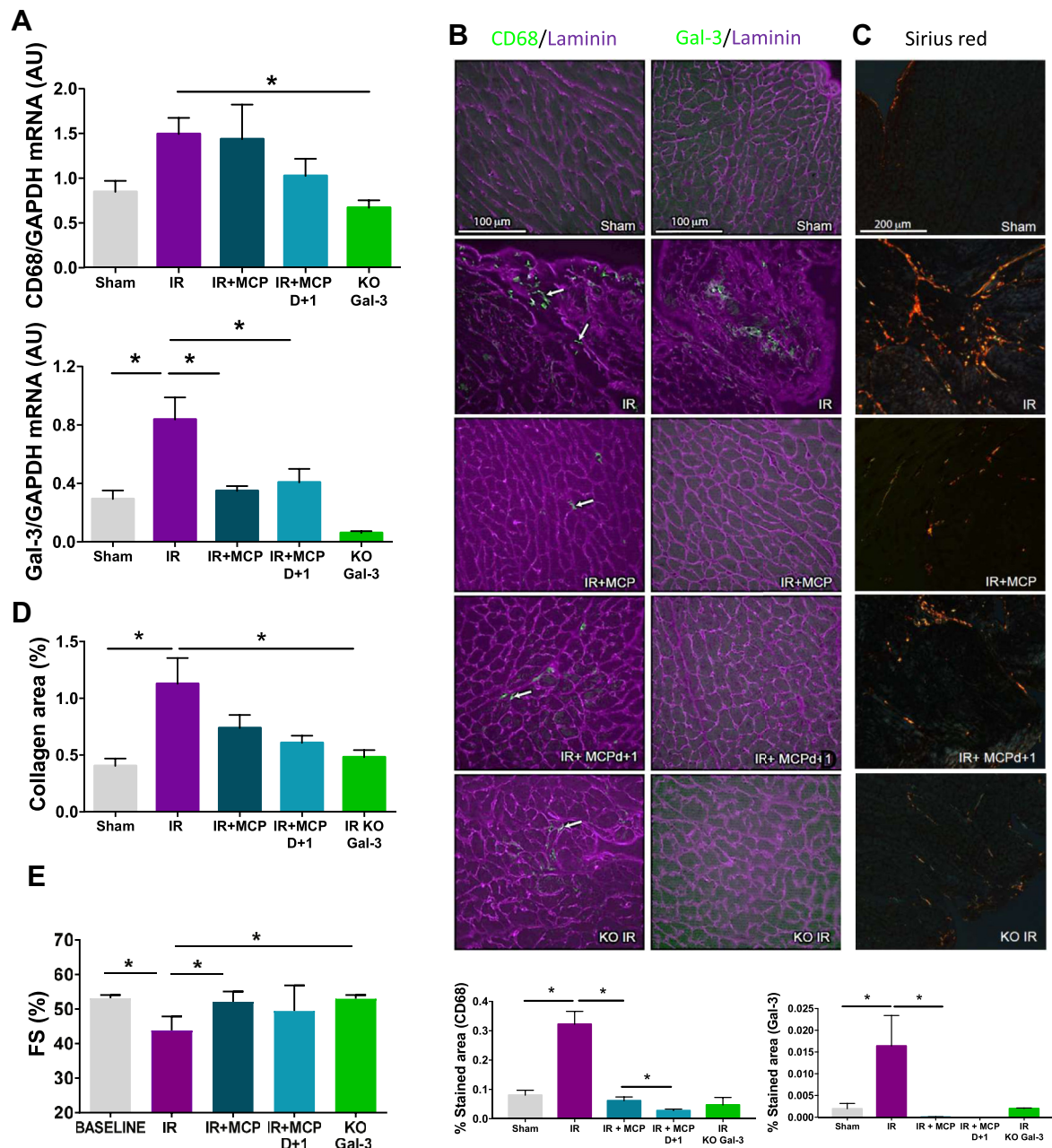
HUMAN COHORT. The association among AKI, Gal-3, and cardiac injury was explored in the FROG-ICU (French and European Outcome Registry in Intensive Care Units) (NCT01367093). This study was an international observational study that included consecutive critically ill patients admitted to 23 intensive care units (ICUs) who received mechanical ventilation and/or vasopressors. The protocol was previously described elsewhere (15). In this

subanalysis, patients with chronic kidney disease were excluded. The study population included 1,110 patients discharged from ICUs with neutrophil gelatinase-associated lipocalin data available on ICU admission and Gal-3 data available at ICU discharge. AKI was defined by the Kidney Disease Improving Global Outcome (KDIGO) definition (clinical AKI) or neutrophil gelatinase-associated lipocalin >150 ng/ml at ICU admission (subclinical AKI) (16,17). Plasmatic levels of cardiac injury and/or stress biomarkers were measured at ICU discharge (plasma Gal-3, N-terminal-pro-brain natriuretic peptide [NT-proBNP], and high-sensitivity troponin level). Interleukin (IL)-6 was measured as a biomarker of systemic inflammation.

STATISTICAL ANALYSIS. The primary endpoint was the association between Gal-3 expression and AKI. Results are expressed as mean ± SEM. A nonparametric Mann-Whitney U test was performed, unless otherwise stated. Levels of Gal-3 at discharge were compared using the Kruskal-Wallis test in the clinical cohort. Univariable and multivariable analyses using propensity score matching assessed the association between AKI and Gal-3 at ICU discharge in the clinical cohort. Variables included in the multivariable analysis were age, hypertension, chronic kidney disease, atrial fibrillation, liver disease, chronic heart failure, dyslipidemia, vascular disease, cancer, body mass index, heart rate, chronic obstructive pulmonary disease, Charlson score, simplified organ failure assessment score, simplified acute physiology score of 2, inotrope use, estimated glomerular filtration rate (eGFR) (using the Modified and Diet Renal Disease formula), septic shock, use of red blood cell transfusion, length of stay in the ICU, sex, and arterial blood pressure. Propensity score matching considered the probability that a patient with specific baseline characteristics had an AKI and then allowed

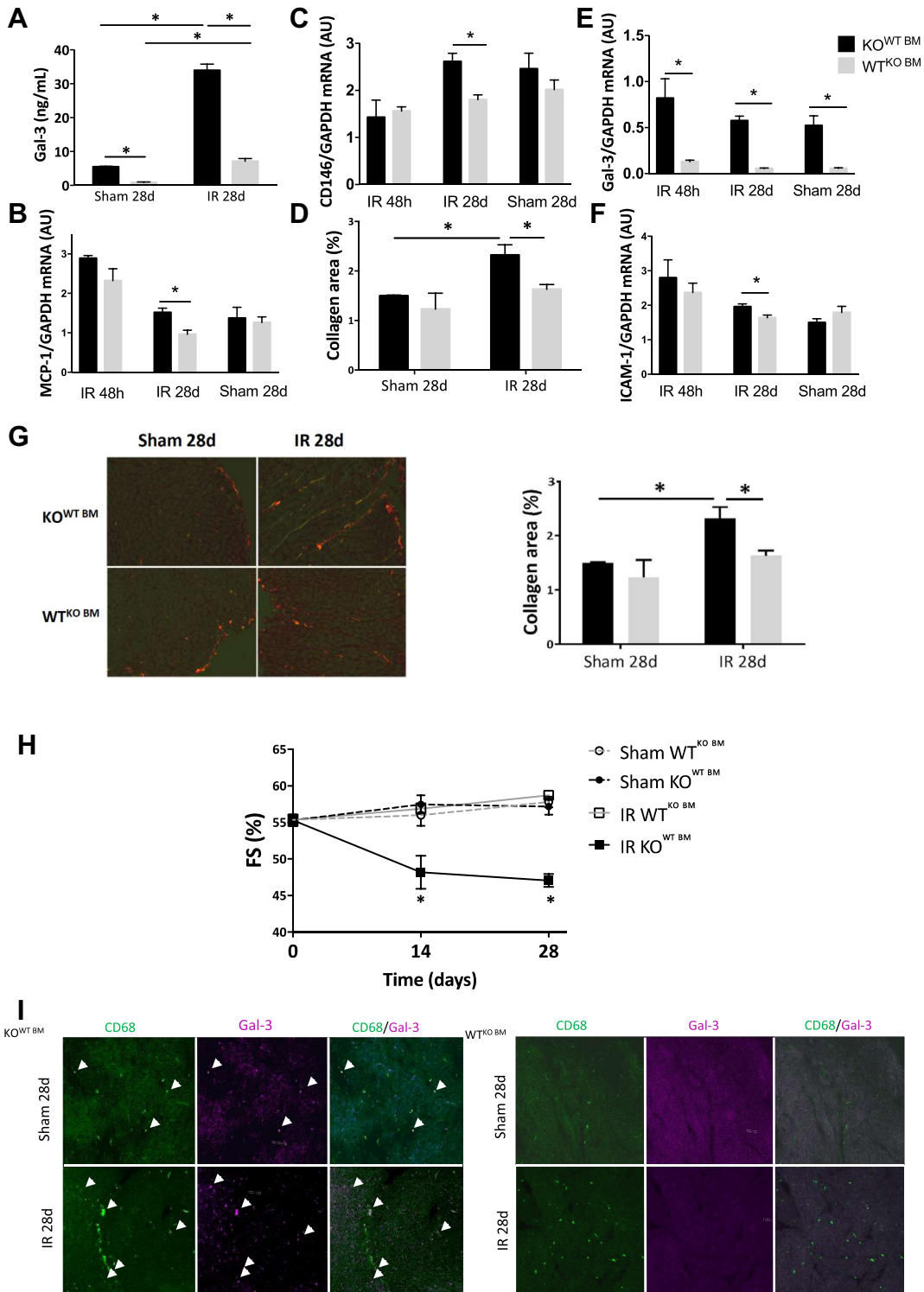
FIGURE 2 Continued

(A) Superposition of Gal-3 mRNA expression kinetics in the kidney and heart showed an early increase in Gal-3 in the kidney ($p < 0.001$; 24 h vs. 0 h), which preceded similar observations in the heart ($p < 0.001$; 48 h vs. 6 h). (B) Cardiac Gal-3 protein quantification confirmed this result, and increased cardiac Gal-3 levels were observed at 72 h compared with the sham group ($p = 0.016$). (C) Kidney Gal-3 protein levels after IR. (D) Gal-3 plasma levels began to increase at 48 h after IR compared with the sham group ($p = 0.037$), peaked at 72 h ($p = 0.017$ for WT IR mice vs. WT sham mice), and remained higher for 28 days compared with the sham group and modified citrus pectin (MCP)-treated mice ($p < 0.001$). (E) Cardiac CD68 mRNA increased at 48 h in WT IR mice ($p = 0.017$ vs. sham group) and was significantly higher than that in Gal-3 KO mice ($p = 0.03$). (F) CD68 immunostaining revealed positive cells at 72 h after reperfusion in IR mice compared with sham mice. Quantification confirmed increased Gal-3 expression in the heart. (G) Cytokine assays performed in plasma from WT (sham, IR, IR+MCP and IR+MCP d+1) and Gal-3 KO mice (sham and IR) showed a significant increase in interleukin (IL)-1- β , IL-6, IL-10, and tumor necrosis factor (TNF)- α levels at 6 and 48 h in WT IR mice, compared with WT IR+MCP ($p < 0.001$), KO IR ($p < 0.001$), and WT sham mice ($p < 0.001$). For A, $n = 4$ to 14. For B and C, $n = 4$ to 7 for the WT and sham groups. For E and G, $n = 4$ for sham, $n = 7$ to 14 for WT IR, $n = 7$ to 12 for WT IR + MCP, $n = 4$ to 7 for KO Gal-3 IR. Data are presented as mean ± SEM, and comparisons of medians were made with the nonparametric Mann-Whitney U test. * $p < 0.05$. GADPH = glyceraldehyde 3-phosphate dehydrogenase; other abbreviations as in Figure 1.

FIGURE 3 At 28 Days, Kidney IR-Induced Cardiac Inflammation and Fibrosis Were Prevented in MCP-Treated and Gal-3 KO Mice

(A) Compared with the IR group, Gal-3 KO mice exhibited blunted cardiac inflammatory responses as indicated by lower CD68 mRNA in KO Gal-3 mice ($p = 0.007$). At 28 days, cardiac expression of Gal-3 remained high versus sham ($p = 0.028$). Mice treated with MCP had a lower cardiac expression of Gal-3 ($p = 0.008$ for WT IR vs. WT IR+MCP, and $p = 0.04$ for WT IR vs. WT IR+MCP day + 1 [d+1] comparisons). (B) Similar results were obtained after cardiac CD68 immunolabeling. CD68+ cells (green) were present in IR mice, whereas Gal-3 KO and MCP-treated mice showed the minimum CD68+ cells. Cardiac Gal-3 immunolabeling was positive in IR hearts but negative in treated mice. Quantification of Gal-3 and CD68 immunostainings confirmed the preceding observations ($p = 0.012$ for WT IR vs. WT IR+MCP and $p < 0.001$ for WT IR vs. WT IR+MCP d+1 for CD68 immunostaining comparisons; $p < 0.001$ for both comparison WT IR vs. IR+MCP and WT IR vs. WT IR+MCP d+1 for Gal-3 immunostaining comparisons). (C) Sirius red coloration of the IR hearts treated with MCP (IR+MCP and IR+MCP d+1) and in Gal-3 KO mice revealed limited cardiac fibrosis. (D) Computer-assisted cardiac fibrosis evaluation confirmed these results ($p < 0.001$ for WT sham vs. WT IR and $p = 0.003$ for WT IR vs. KO Gal-3 IR). (E) Cardiac function assessed by the analysis of left ventricular fractional shortening (FS) was altered in response to IR ($p < 0.001$ baseline vs. IR) and rescued in KO-treated mice ($p = 0.002$ for IR vs. IR+MCP and $p < 0.001$ for IR vs. KO Gal-3). For A to C, $n = 5$ for sham group, $n = 7$ to 10 for WT IR, $n = 5$ to 6 for WT IR+MCP, $n = 5$ to 6 for WT IR+MCP d+1, and $n = 5$ to 8 for KO Gal-3 IR. For E, $n = 43$ for baseline echography and $n = 7$ for other groups. Data are presented as mean \pm SEM and comparisons of medians were made with the nonparametric Mann-Whitney U test. * $p < 0.05$. Abbreviations as in Figures 1 and 2.

FIGURE 4 Gal-3 From BM-derived Cells, Including Macrophages, Is Sufficient to Induce Cardiac Fibrosis and Dysfunction



Continued on the next page

the comparison of Gal-3 levels in patients with or without AKI but with similar characteristics. The propensity score model included age, hypertension, chronic kidney disease, atrial fibrillation, liver disease, chronic heart failure, dyslipidemia, vascular disease, cancer, body mass index, heart rate, chronic obstructive pulmonary disease, Charlson score, simplified organ failure assessment score, simplified acute physiology score of 2, inotrope use, renal replacement therapy, eGFR (using the Modified and Diet Renal Disease formula), septic shock at admission, use of red blood cell transfusion during ICU stay, length of stay in the ICU, sex, and arterial blood pressure. Matching was performed according to the nearest neighbor approach within a caliper width of 0.2 (18). Imbalance between patients with and without AKI before and after propensity score matching was assessed using a standardized difference, considering <10% acceptable to define the study patients' characteristics balanced with respect to the previously described features. All statistical analyses were performed using R statistical software version 3.1.1 or above (The "R" Foundation for Statistical Computing, Vienna, Austria). A p value <0.05 was considered statistically significant.

RESULTS

AKI INDUCES GAL-3 EXPRESSION, CARDIAC INJURY, AND SYSTEMIC INFLAMMATION. After renal IR in WT mice, a transient increase in creatinine (Cr) and blood urea nitrogen (BUN) levels was observed 24 h post-reperfusion (Figure 1A). Cr and BUN returned to baseline within 48 h.

AKI induced an increase in kidney Gal-3 expression, mainly in tubular cells and monocytes at 24 h (Figures 1B to 1D). The increased expression of Gal-3 in

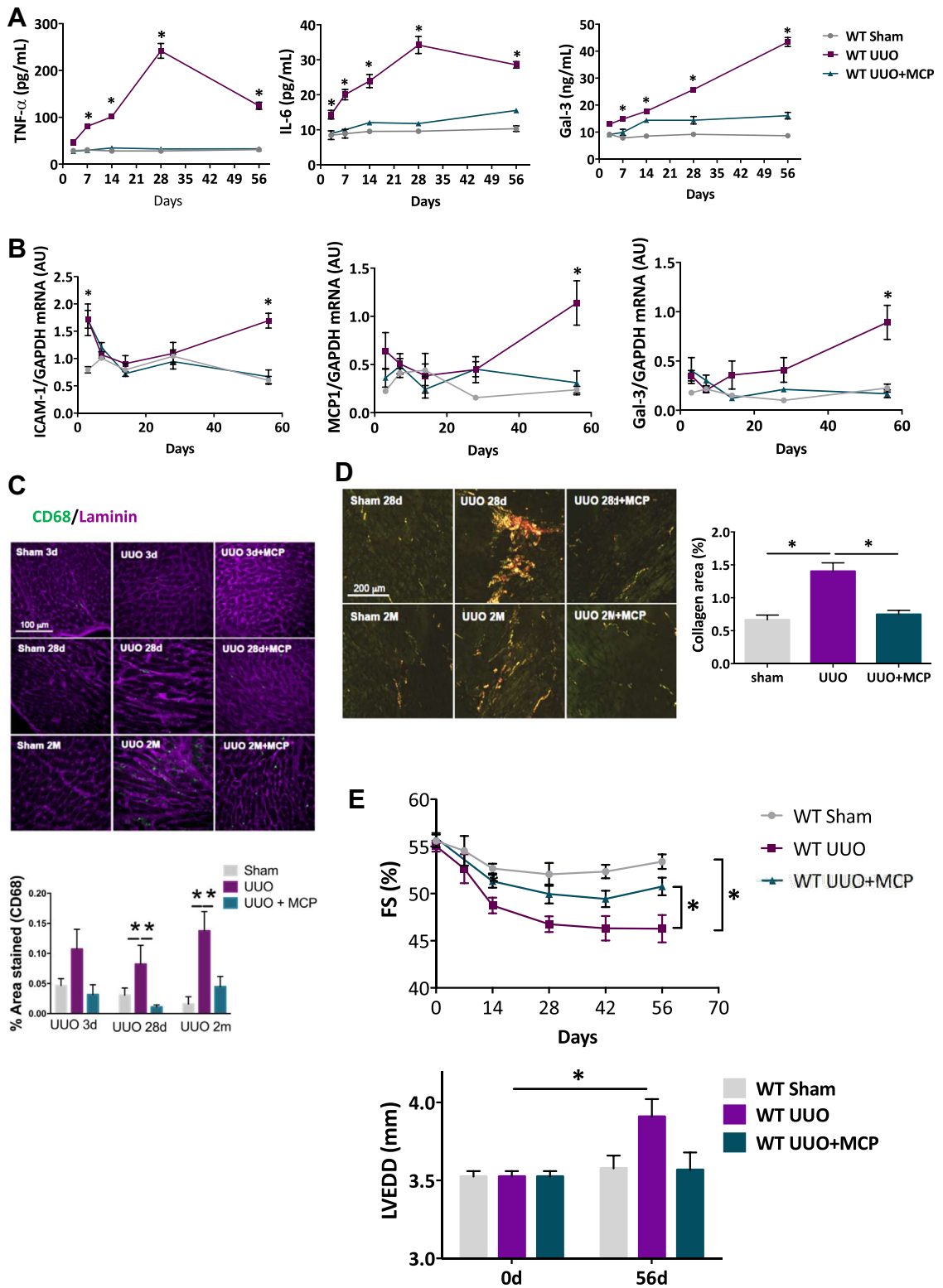
monocytes was also confirmed in isolated renal macrophages (Supplemental Figure 3). This increase was followed by an increase in cardiac Gal-3 expression at 48 h (Figure 2A), which was confirmed at the protein level (Figures 2B and 2C). Cardiac tissue infiltration by inflammatory cells and systemic inflammation assessed with plasma cytokines and adhesion molecule levels measurements were observed during the first 72 h after IR. Plasma levels of Gal-3 increased, with a peak at 72 h, and remained elevated until day 28 (Figure 2D). *CD68* mRNA expression increased in the heart at 48 h (Figure 2E). Furthermore, hearts showed *CD68*⁺ cells (infiltrating macrophages) (Figure 2F) and increased *MCP-1* mRNA expression at 72 h post IR versus that in sham mice (1.49 ± 1.0 vs. 4.1 ± 1.8 ; $p < 0.001$). Cytokines assays performed on plasma showed an increase in IL-1 β , IL-6, IL-10, and tumor necrosis factor (TNF)- α levels at 6 and 48 h after IR (Figure 2G). Furthermore, adhesion of monocytes on endothelial monolayers was significantly increased after stimulation with recombinant Gal-3 (Supplemental Figure 4). Twenty-eight days after AKI, cardiac inflammation and fibrosis were observed. mRNA expression of both *CD68* and Gal-3 was increased (Figure 3A). Furthermore, *CD68*⁺ and Gal-3⁺ cells (Figure 3B) and increased collagen areas (Figures 3C and 3D) were observed.

Although cardiac function was normal during the first 72 h, IR induced a late increase in left ventricular diastolic diameter (Supplemental Table 1) and a decrease in fractional shortening (Figure 3E) 28 days after injury. At the anatomical level, kidney hypertrophy was observed 28 days after AKI and was not prevented by MCP treatment (Supplemental Table 1). Hind limb ischemia did not lead to cardiac dysfunction and injury, or changes in Gal-3 expression (Supplemental Figure 5).

FIGURE 4 Continued

(A) Plasmatic assays from chimeric mice *WT*^{KO BM} mice (WT mice grafted with Gal-3 KO bone marrow [BM]) and *KO*^{WT BM} mice (Gal-3 KO mice grafted with WT bone marrow) showed a difference in plasmatic Gal-3 level between sham *WT*^{KO BM} and sham *KO*^{WT BM} mice at 28 days. Furthermore, in response to IR, Gal-3 level was highly increased at 28 days post-IR in *KO*^{WT BM} mice compared with sham mice ($p = 0.016$), whereas in *WT*^{KO BM} mice, the Gal-3 increase was lower at 28 days post-IR ($p < 0.001$). Gal-3 level was lower in *WT*^{KO BM} mice compared with *KO*^{WT BM} mice ($p < 0.001$). **(B to F)** Interleukine (IL)-6 Cardiac CD146, monocyte chemoattractant protein (MCP)-1, Gal-3 and intercellular adhesion molecule (ICAM)-1 mRNAs expression were analyzed. CD146 and MCP-1 mRNA expression was higher in IR *KO*^{WT BM} mice compare with IR *WT*^{KO BM} mice ($p = 0.001$ for CD146, $p = 0.005$ for MCP-1). Gal-3 mRNA level did not alter in response to IR, but the level in *KO*^{WT BM} mice was increased 6-fold vs *WT*^{KO BM} mice ($*p < 0.001$ for all comparisons). **(G)** Sirius red coloration showed an increase in collagen fibers in response to IR in *KO*^{WT BM} mice and blunted in *WT*^{KO BM} mice. Computer-assisted cardiac fibrosis evaluation confirmed these results. **(H)** Echocardiography revealed a decline in fractional shortening after 28 days post-IR in *KO*^{WT BM} mice that was prevented in *WT*^{KO BM} mice ($p < 0.001$ for IR *KO*^{WT BM} mice vs. IR *WT*^{KO BM} mice at 14 and 28 days) **(I)** CD68/Gal-3 co-immunostaining performed on *WT*^{KO BM} mice and *KO*^{WT BM} mice showed CD68+ (green)/Gal-3+ (purple) cells in *KO*^{WT BM} mice. CD68 staining appeared to be more important and grouped after acute kidney injury. No Gal-3 staining was observed in *WT*^{KO BM} mice despite CD68+ cells in sham and IR mice. For 48 h and 28 days, $n = 4$ for sham *KO*^{WT BM} mice, $n = 5$ for sham *WT*^{KO BM} mice, $n = 5$ for IR *KO*^{WT BM} mice, $n = 9$ for IR *WT*^{KO BM} mice. Data are presented as mean \pm SEM and comparisons of medians were made with the nonparametric Mann-Whitney U test. $*p < 0.05$. Abbreviations as in Figure 1.

FIGURE 5 Unilateral Ureteral Obstruction Leads to Cytokines Release, Cardiac Inflammation, Fibrosis and Dysfunction, Which Is Prevented in MCP Treated Mice



AKI-INDUCED CARDIAC INFLAMMATION, FIBROSIS, AND DYSFUNCTION IS GAL-3 DEPENDENT. Inactivation of Gal-3 by pharmacological inhibition (MCP treatment) and by genetic invalidation (Gal-3 KO mice) blunted cardiac consequences of AKI. Gal-3 inactivation prevented Gal-3 and cytokine release (Figures 2D and 2G), as well as cardiac endothelial activation (Figure 2H) during the first 72 h after renal IR. At 28 days post-AKI, Gal-3 inactivation prevented cardiac monocyte recruitment, Gal-3 increase (Figure 3B), cardiac fibrosis, and cardiac dysfunction (Figures 3C to 3E).

GAL-3 FROM BM-DERIVED CELLS IS RESPONSIBLE FOR CARDIAC DAMAGE. AKI was performed in a graft mouse model of BM. Chimeric mice were submitted to renal IR and killed 28 days post-reperfusion (Supplemental Figures 1B and 2). No variations in anatomical data were observed (Supplemental Table 2). Plasma Gal-3 levels were close to zero in sham WT^{KO BM} mice. Furthermore, in response to renal IR, plasma Gal-3 levels were higher in KO^{WT BM} than in WT^{KO BM} mice (Figure 4A). No variation in plasmatic IL-6 levels was observed at 28 days post-IR (Figure 4B). Cardiac *CD146* and *MCP-1* mRNA levels, an endothelial and inflammatory marker, respectively, were lower in IR WT^{KO BM} mice versus KO^{WT BM} mice (Figures 4C and 4D). Cardiac *Gal-3* mRNA expression did not change between sham and IR mice but varied according to mice genotype. However, Gal-3 protein expression was slightly increased at 28 days after IR (Supplemental Figure 6). Cardiac Gal-3 mRNA expression was higher in KO^{WT BM} mice than in WT^{KO BM} mice (Figure 4E). Moreover, an increase in *ICAM-1* mRNA expression was observed in response to IR only in KO^{WT BM} mice (Figure 4F). Furthermore, Sirius red staining showed a significant increase in cardiac interstitial fibrosis in response to IR in KO^{WT BM} mice compared with sham mice, which was blunted in WT^{KO BM} mice (Figure 4G).

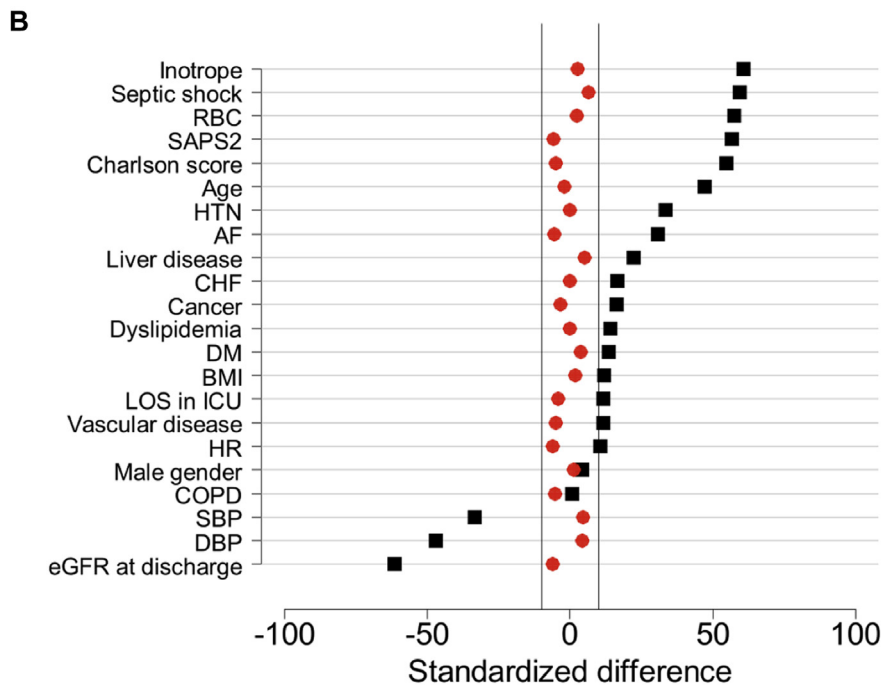
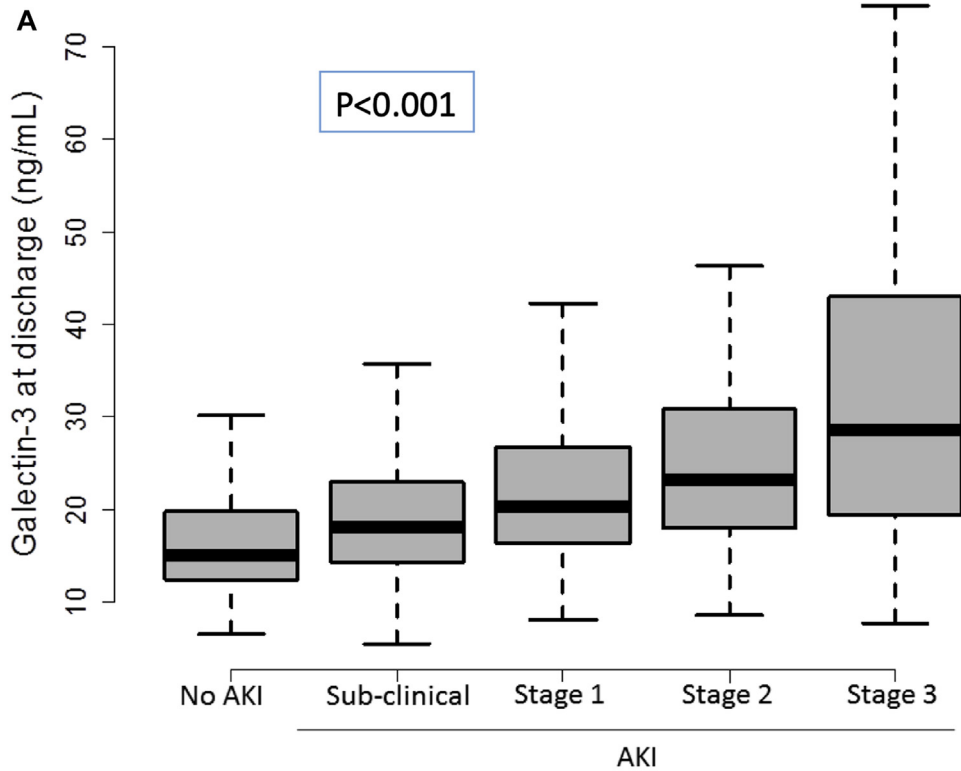
Echocardiography revealed a decrease in fractional shortening after IR only in KO^{WT BM} mice (Figure 4H). Finally, CD68/Gal-3 co-staining in cardiac tissue showed CD68⁺/Gal-3⁺ cells in KO^{WT BM} mice, whereas CD68⁺ cells in WT^{KO BM} mice were Gal-3⁻ (Figure 4I).

CARDIAC DAMAGE AFTER AKI IS GAL-3 DEPENDENT BUT RENAL FUNCTION INDEPENDENT. Next, we assessed another model of renal injury, the unilateral ureteral obstruction (UUO), which does not affect renal function (Supplemental Figures 7A and 7B). Levels of Cr and BUN remained normal after UUO, whereas inflammation increased in the obstructed kidney. UUO+MCP mice were protected against renal inflammation (Supplemental Figure 7B). An increase in tubular dilatation was observed in both UUO and UUO+MCP mice at 15 days; an increase in right kidney weight (i.e., renal hypertrophy) was also observed at 2 months (Supplemental Figure 7B, Supplemental Table 3). Plasma levels of TNF- α , IL-6, IL-1 β , and IL-10 were also increased after UUO and peaked at 28 days, except for IL-1 β , which rapidly increased after surgery, peaked at 7 days, and then decreased and returned to baseline. The increase of cytokine levels was prevented by MCP treatment (Figure 5A, Supplemental Figure 8). Plasma levels of Gal-3 increased progressively during the 2 months of UUO (by 4-fold compared with sham group). In MCP-treated mice, the plasmatic increase of Gal-3 was blunted (Figure 5A). Similar signs of cardiac damage were observed compared with the renal IR model. An early (day 3) and transient cardiac increase in *ICAM-1* and late (2 months) increase in *ICAM-1*, *MCP-1*, and Gal-3 mRNA levels were observed in response to UUO, which were all prevented by MCP treatment (Figure 5B). At 28 days and 2 months, UUO induced cardiac inflammation and fibrosis, as shown by CD68⁺ cells (Figure 5C) and by an increase of interstitial collagen areas (Figure 5D). MCP treatment prevented fibrosis (Figures 5C and 5D). Importantly, UUO

FIGURE 5 Continued

(A) Cytokine assays performed in plasma showed a progressive increase in TNF- α , IL-6, and gal-3 levels until 28 days and 2 months respectively in response to UUO compared to WT UUO+MCP ($p < 0.001$ for comparisons at 28 days and 56 days) and WT sham mice ($p < 0.001$ for comparisons at 28 days and 56 days). (B) In response to UUO, cardiac mRNAs increased expressions of *ICAM-1*, *MCP-1* and gal-3 compared to sham (UUO vs sham: $p < 0.001$ for *ICAM-1*, $p = 0.019$ for *MCP-1*, $p = 0.024$ for gal-3) were prevented in MCP treated mice at 2 months post-surgery (for UUO vs UUO+MCP: $p = 0.002$ for *ICAM-1*, $p < 0.001$ for *MCP-1*, $p = 0.002$ for gal-3). (C) CD68/Laminin immunostaining performed on cardiac tissue showed an increase in CD68⁺ cells in response to UUO from 28 days and less CD68⁺ cells in UUO+MCP. Quantification of CD68 staining confirmed the above observations. ($p = 0.047$ for UUO vs sham and $p = 0.01$ for UUO vs UUO+MCP at 28 days; $p = 0.035$ for UUO vs sham and $p = 0.011$ for UUO vs UUO+MCP at 2 months). (D) Sirius red coloration revealed cardiac fibrosis after 2 months of UUO. MCP treatment blunted collagen accumulation and deposition. Computer-assisted cardiac fibrosis evaluation confirmed these results ($p < 0.001$ for both comparisons UUO vs sham and UUO vs UUO+MCP). (E) Left ventricular Fractional shortening (FS) analysis by echocardiography after 2 months highlights a progressive decreasing in FS in response to UUO ($p = 0.01$ for UUO vs sham), prevented in treated mice ($p = 0.02$ for UUO vs UUO+MCP). Left ventricular end diastolic diameter (LVEDD) analysis revealed an increase in LVEDD after 2 months for UUO ($p = 0.043$ UUO vs sham), reflecting left ventricular dilatation. For different time points, $n = 4$ for WT sham UUO, $n = 5-8$ for WT UUO, $n = 6-8$ for WT UUO + MCP. Data are presented as mean \pm SEM and comparisons of medians were made with non-parametric Mann-Whitney U test. * $p < 0.05$. Abbreviations as in Figures 1, 2, and 4.

FIGURE 6 Plasma Gal-3 and AKI in Critically Ill Patients Discharged From ICU



(A) Plasma Gal-3 level at hospital discharge according to AKI stage (sub-clinical, and stage 1, 2, or 3 of the KDIGO guidelines). We observed a stepwise increase of plasma Gal-3 level with AKI stages. **(B)** Graphical representation of imbalance in patients' characteristics before and after propensity score (PS) matching between no AKI and AKI patients (**Black squares** represents mean standardized difference [MSD] before PS-matching and the **red points** MSD after PS-matching). Abbreviations as in [Figure 1](#).

induced left ventricular dilatation and a decrease in fractional shortening, which was prevented by MCP (Figure 5E).

AKI IS ASSOCIATED WITH GAL-3 EXPRESSION AND CARDIAC INJURY AT ICU DISCHARGE IN THE CLINICAL SETTING. In the clinical cohort, 645 (58%) patients developed AKI during ICU stay and were discharged alive (Supplemental Table 4), including 252 patients with subclinical AKI and 134, 65, and 194 patients with AKI KDIGO stages 1, 2, and 3, respectively. Plasma level of Gal-3 showed a stepwise increase with severity of AKI (from subclinical to stage 3) (Figure 6). Plasma level of Gal-3 was associated with AKI in univariable analysis (mean difference: 8.60 ng/ml; 95% CI: 7.04 to 10.15; $p < 0.001$) and remained significantly associated after adjustment for confounding factors in multivariable analysis (mean difference: 5.13 ng/ml; 95% CI: 2.92 to 7.35; $p < 0.001$). AKI was associated with increased biomarkers of cardiac injury (Gal-3, sST-2 and high-sensitivity troponin I), increased cardiac stress (NT-proBNP), and systemic inflammation (IL-6) at ICU discharge, even in patients who recovered their renal function (Supplemental Table 5).

DISCUSSION

In this study, we explored the impact of AKI on remote cardiac injury. Results showed that renal IR promoted the development of cardiac injury and fibrosis in part through the activation of the Gal-3 pathway. Gal-3 originated from BM-derived cells, including macrophages. Furthermore, by using the UUO model of renal disease we showed that cardiac injury occurred after renal damage even if renal function was not affected. Altogether, our data indicated that the activation of the Gal-3 pathway represents 1 of the causal links between AKI and cardiac injury.

Our findings provided important insights into cardiorenal syndrome type 3 or acute reno-cardiac syndrome (AKI leading to cardiac injury) pathophysiology (19). We hypothesized that AKI triggers the secretion of Gal-3, which promotes the development of cardiac injury by generating fibrosis.

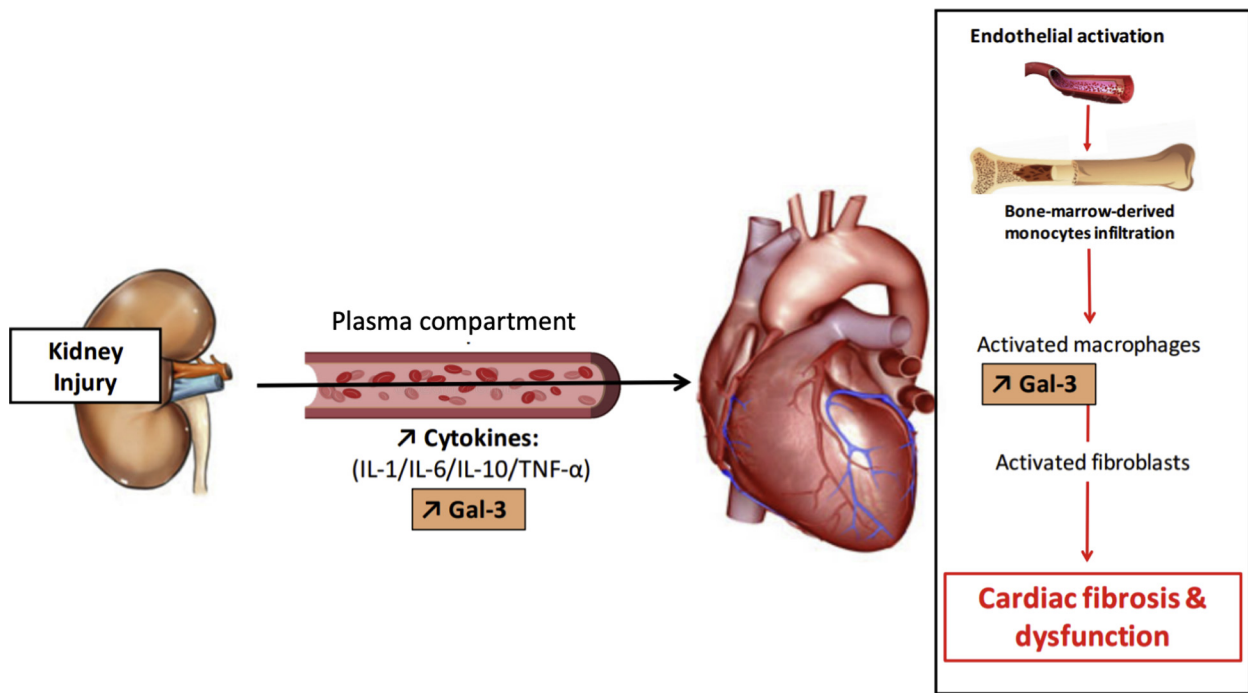
Occurrence of AKI was associated with both short- and long-term risk of mortality in different settings (1). Furthermore, there was increasing evidence that AKI is associated with a risk of cardiovascular events (3,20). Recently, Go et al. (21) explored the association between AKI and the risk of cardiovascular events during the year following hospital discharge. Using a large database with propensity score matching, they

observed that AKI was a risk factor for heart failure during the year following discharge. Such cardiovascular consequences of AKI may be causal (at least partially) in the poor outcomes of the injury. In this study, we explored the association between AKI and circulating expression of Gal-3 and cardiac injury in critically ill patients. We observed that patients who presented with AKI during ICU stay and survived had higher plasma Gal-3 levels at discharge, along with high plasma levels of biomarkers of cardiac injury and failure. Although renal function did affect the level of natriuretic peptides and troponin, eGFR did not appear to be the major determinant of these cardiac biomarker levels (22). Recent data showed similar diurnal variation in patients with and without chronic kidney disease, which suggested that decreased clearance is not the primary mechanism for elevated high-sensitivity cardiac troponin levels in the patients with renal failure (23). Importantly, elevated levels of natriuretic peptides and troponin were associated in many studies with cardiovascular events and outcome (24,25). Therefore, these biomarkers are still considered valid biomarkers of cardiovascular events in patients with renal failure. Finally, patients with AKI but who were discharged with eGFR >60 ml/min/1.73 m² showed elevated plasma biomarkers of cardiac damage compared with patients without AKI (Supplemental Table 5).

We used preclinical models to explore the pathophysiological roles of Gal-3 after AKI. In our models, acute cardiac response to renal injury was characterized by an early increase in plasmatic cytokine levels and cardiac injury. The acute cardiac response was followed by a late cardiac response that was characterized by systolic dysfunction and cardiac fibrosis. The early and late cardiac responses were Gal-3-dependent because they were prevented by MCP, a Gal-3 inhibitor, and in Gal-3 KO mice. Of note, the role of Gal-3 in remote cardiac injury was specifically linked to renal injury because hind limb IR did not induce any cardiac damage. Furthermore, Gal-3 remained elevated both in the plasma and heart in the preclinical models despite complete restoration of renal function.

In short-term animal experiments, AKI was shown to promote cellular apoptosis in the heart, followed by cardiac hypertrophy and fibrosis. Burchill et al. (26) observed cardiac hypertrophy and fibrosis 10 days after renal IR. Increased levels of immunoreactive *TNF- α* , *IL-1*, and *ICAM-1* mRNA were also reported in the heart within 48 h after renal IR (27). Furthermore, cardiomyocyte apoptosis was also observed and associated with cardiac dysfunction evaluated by

FIGURE 7 Schematic Representation of the Results From Initial Renal Injury to Cardiac Dysfunction, Including the Effects of Gal-3 Inhibition



Renal injury induced transient renal dysfunction only in the IR model (increase in creatinine and blood urea nitrogen), as well as tubular cell response and macrophage activation, which led to an increase in Gal-3 expression. These features led to systemic inflammation by increasing levels of plasma cytokines (IL-1, IL-6, IL-10, and TNF- α) and Gal-3, which induced cardiac endothelial activation as shown by increased in ICAM-1, vascular cell adhesion molecule-1, monocyte chemoattractant protein-1 and connective tissue growth factor mRNA levels. Endothelial activation promoted monocyte infiltration in cardiac tissue; these monocytes differentiated into activated macrophages (increased CD68), thus expressing and secreting transforming growth factor (TGF)- β and Gal-3. TGF- β and Gal-3 may participate in the activation of fibroblasts leading to collagen type 1 and 3 synthesis and subsequent cardiac fibrosis and dysfunction. Treatment with MCP, Gal-3 deletion (Gal-3 KO mice), and WT mice grafted with Gal-3 KO BM, prevented the increase in plasma cytokines, Gal-3, cardiac Gal-3, fibroblast activation, and the increase in cardiac fibrosis, which therefore prevented cardiac dysfunction. Abbreviations as in [Figures 1, 2, and 4](#).

echocardiography at 72 h (28). In another study, the macrophage chemokine osteopontin was increased, along with macrophage infiltration in the heart after 24 h of renal IR (29). In addition, increased TNF- α , IL-6, and IL-1 β plasma concentrations were observed 3 h after renal IR (30). In our model, cytokine assays showed increased plasma cytokine levels in response to AKI during the acute stage (6 to 48 h). This increase was prevented in MCP-treated and Gal-3 KO mice. Martinez-Martinez et al. (8) showed that experimental hyperaldosteronism leads to cardiac fibrosis in a Gal-3-dependent pathway that is independent of blood pressure (8). The results from our study showed that AKI promoted Gal-3-dependent cardiac injury and inflammation, fibrosis, and systolic dysfunction.

Recently, macrophages were identified as key players in the development of heart failure (31). As we observed in our model, infiltration of macrophages

was facilitated by the activation of the endothelium (which overexpresses its cell surface adhesion proteins, intercellular adhesion molecule-1, vascular cell adhesion molecule-1), which favored inflammatory cells transfer from the vascular compartment to the tissue. The role of Gal-3 as a chemokine was previously shown by Sano et al. (32), and in addition to that study, we showed that Gal-3 promotes monocyte adhesion (Supplemental Figure 4). Consequently, Gal-3 might have both chemoattractive and pro-adhesive effects locally in the damaged tissues. Gal-3 was already known for inducing fibrosis via the synthesis of TGF- β (33), but also by activating fibroblasts and collagen synthesis (34). The pro-fibrotic effect of Gal-3 was observed separately both in the kidney and the heart, making this lectin a serious promoter of type 3 cardiorenal syndrome. MCP is a complex water-soluble indigestible polysaccharide rich in β -galactose. The

carbohydrate chains of MCP are rich in galactose and are recognized by Gal-3 carbohydrate recognition domains. MCP's recognized mode of action is Gal-3 activity inhibition via carbohydrate recognition domains. There are currently no data that show anti-cytokinic or pro-cytokinic action of MCP via another pathway. However, we could not confirm the specificity of the carbohydrate recognition domain pathway mechanism of action of MCP.

AKI can induce systemic sympathetic nervous system and renin-angiotensin-aldosterone system activation (35). Although the increase in systemic arterial pressure was not sustained, increased vascular reactivity to angiotensin II was reported (36). Our group and others showed that activation of the renin-angiotensin-aldosterone system could promote cardiac and renal injuries (10,11). Gal-3 participates in the mechanisms of aldosterone-mediated myocardial damage. It is therefore also possible that activation of the renin-angiotensin-aldosterone system promotes endothelial injury in remote organs after AKI. These vascular consequences should be investigated in the future.

Finally, cardiac fibrosis has been extensively recognized as a key player in the development of heart failure. In our models, cardiac expression of Gal-3 was decreased in mice that received MCP compared with control mice and was associated with lower macrophage infiltration, which reflected a possible positive feedback of Gal-3 on macrophage recruitment. Thus, a decrease in cardiac Gal-3 expression may arise from direct synthesis inhibition as well as a decrease in macrophage recruitment.

We explored the source of Gal-3 in our models. Gal-3 can be expressed in different cell types including tubular and immune cells (37). In our model of renal IR, damaged tubules expressed Gal-3 and might also be the source of pro-inflammatory cytokine expression. In this study, the question of the source of cardiac Gal-3 after AKI was mainly explored using BM transplantation. We showed that renal IR led to an increase in Gal-3 expression, cardiac fibrosis, and dysfunction in WT mice, but this damage was prevented in WT^{KO BM} mice. Furthermore, we observed cardiac CD68+/Gal-3+ cells by immunostaining only in KO^{WT BM} mice, whereas WT^{KO BM} mice did not express cardiac Gal-3. This set of experiments confirmed that cardiac Gal-3 arises from BM-derived immune cells, including macrophages. Souza et al. (38) showed in a mouse model of myocarditis that cardiac Gal-3 expression was high in macrophages, T cells, and fibroblasts using flux cytometry and

confocal microscopy. Inhibition of Gal-3 by MCP or N-acetyl-D-lactosamine reduced cardiac inflammation and fibrosis and modulated the expression of pro-inflammatory genes in the heart.

Gal-3 appears to be a mandatory mediator for AKI-Induced cardiac damage because a specific blockage of the Gal-3 pathway prevented cardiac damage and injury. Gal-3 was shown to trigger immune cells and cytokines release. Inhibition of Gal-3 activity led to inhibition of macrophage recruitment and activation, and therefore, indirectly to a decrease in cytokine expression (e.g., TNF- α , IL-1, IL-6, IL-4, or IL-8 (34,39)). The decrease in the expression of these cytokines led to the modulation of other cytokines in the downstream inflammatory cascade. Therefore, Gal-3 appeared upstream of the release of these cytokines. However, it remains to be tested whether blocking 1 of these downstream cytokines (IL-1, IL-6, TNF- α) would have cardioprotective effects as well.

A summary scheme of our results is shown in **Figure 7**. Kidney injury induces an increase in renal, circulating, and cardiac Gal-3 expression and in circulating cytokines levels. Kidney injury leads to cardiac damage via endothelium activation, monocyte recruitment, and finally development of cardiac fibrosis and dysfunction. Remote cardiac consequences of kidney injury are prevented in Gal-3 KO mice, MCP-treated mice, and in WT^{KO BM} mice.

CONCLUSIONS

The Gal-3 pathway is involved in remote cardiac damage after AKI, which may be involved in AKI-associated poor outcomes. Cardiac Gal-3 originates from BM-derived cells. These findings open an area of clinical research with the aim of prevention of devastating consequences of AKI in humans.

ACKNOWLEDGMENTS The authors thank Pr Hang Korng Ea for discussions and help in Gal-3 KO mice strain development, Merval Régine, Polidano Evelyn, and Placier Sandrine for their technical assistance with the animal model, and Dr. Panagiotis Kavvas for critical reading of the manuscript.

ADDRESS FOR CORRESPONDENCE: Dr. Matthieu M. Legrand, Department of Anesthesiology and Peri-Operative Care, University of California San Francisco, 500 Parnassus Avenue, E410, San Francisco, California 94117. E-mail: matthieu.legrand@ucsf.edu.

PERSPECTIVES

COMPETENCY IN MEDICAL KNOWLEDGE: AKI leads to remote cardiac injuries, including cardiac inflammation, acute dysfunction, and *in fine* fibrosis. These effects may contribute to poor outcomes after AKI. Remote cardiac injury after AKI is in part mediated by a Gal-3–dependant pathway that originates mainly from BM-derived immune cells.

TRANSLATIONAL OUTLOOK: Future research should examine inhibition of the Gal-3 pathway after AKI to prevent the adverse cardiac effects induced by AKI and to improve its prognosis.

REFERENCES

1. Sawhney S, Marks A, Fluck N, Levin A, Prescott G, Black C. Intermediate and long-term outcomes of survivors of acute kidney injury episodes: a large population-based cohort study. *Am J Kidney Dis* 2017;69:18–28.
2. Kaddourah A, Basu RK, Bagshaw SM, Goldstein SL, AWARE Investigators. Epidemiology of acute kidney injury in critically ill children and young adults. *N Engl J Med* 2017;376:11–20.
3. Parikh CR, Puthumana J, Shlipak MG, et al. Relationship of kidney injury biomarkers with long-term cardiovascular outcomes after cardiac surgery. *J Am Soc Nephrol* 2017;28:3699–707.
4. Yap SC, Lee HT. Acute kidney injury and extra-renal organ dysfunction: new concepts and experimental evidence. *Anesthesiology* 2012;116:1139–48.
5. Ronco C, McCullough P, Anker SD, et al. Cardio-renal syndromes: report from the consensus conference of the acute dialysis quality initiative. *Eur Heart J* 2010;31:703–11.
6. Ponikowski P, Voors AA, Anker SD, et al. 2016 ESC Guidelines for the diagnosis and treatment of acute and chronic heart failure: The Task Force for the diagnosis and treatment of acute and chronic heart failure of the European Society of Cardiology (ESC) Developed with the special contribution of the Heart Failure Association (HFA) of the ESC. *Eur Heart J* 2016;37:2129–200.
7. de Boer RA, Voors AA, Muntendam P, van Gilst WH, van Veldhuisen DJ. Galectin-3: a novel mediator of heart failure development and progression. *Eur J Heart Fail* 2009;11:811–7.
8. Martínez-Martínez E, Calvier L, Fernández-Celis A, et al. Galectin-3 blockade inhibits cardiac inflammation and fibrosis in experimental hyperaldosteronism and hypertension. *Hypertension* 2015;66:767–75.
9. Azibani F, Benard L, Schlossarek S, et al. Aldosterone inhibits antifibrotic factors in mouse hypertensive heart. *Hypertension* 2012;59:1179–87.
10. Vergaro G, Prud'homme M, Fazal L, et al. Inhibition of galectin-3 pathway prevents isoproterenol-induced left ventricular dysfunction and fibrosis in mice. *Hypertension* 2016;67:606–12.
11. Calvier L, Martínez-Martínez E, Miana M, et al. The impact of galectin-3 inhibition on aldosterone-induced cardiac and renal injuries. *J Am Coll Cardiol HF* 2015;3:59–67.
12. Dang Z, MacKinnon A, Marson LP, Sethi T. Tubular atrophy and interstitial fibrosis after renal transplantation is dependent on galectin-3. *Transplantation* 2012;93:477–84.
13. Colnot C, Fowles D, Ripoche MA, Bouchaert I, Poirier F. Embryonic implantation in galectin 1/ galectin 3 double mutant mice. *Dev Dyn* 1998;211:306–13.
14. Wei Q, Dong Z. Mouse model of ischemic acute kidney injury: technical notes and tricks. *Am J Physiol Renal Physiol* 2012;303:F1487–94.
15. Mebazaa A, Casadio MC, Azoulay E, et al. Post-ICU discharge and outcome: rationale and methods of the French and euROpean Outcome reGistry in Intensive Care Units (FROG-ICU) observational study. *BMC Anesthesiol* 2015;15:143.
16. Zarbock A, Kellum JA, Schmidt C, et al. Effect of early vs delayed initiation of renal replacement therapy on mortality in critically ill patients with acute kidney injury: the ELAIN randomized clinical trial. *JAMA* 2016;315:2190–9.
17. Ronco C, Legrand M, Goldstein SL, et al. Neutrophil gelatinase-associated lipocalin: ready for routine clinical use? An international perspective. *Blood Purif* 2014;37:271–85.
18. Austin PC. Some methods of propensity-score matching had superior performance to others: results of an empirical investigation and Monte Carlo simulations. *Biom J Biom Z* 2009;51:171–84.
19. Braam B, Joles JA, Danishwar AH, Gaillard CA. Cardio-renal syndrome—current understanding and future perspectives. *Nat Rev Nephrol* 2014;10:48–55.
20. Gammelager H, Christiansen CF, Johansen MB, Tønnesen E, Jespersen B, Sørensen HT. Three-year risk of cardiovascular disease among intensive care patients with acute kidney injury: a population-based cohort study. *Crit Care Lond Engl* 2014;18:492.
21. Go AS, Hsu C-Y, Yang J, et al. Acute kidney injury and risk of heart failure and atherosclerotic events. *Clin J Am Soc Nephrol* 2018;13:833–41.
22. Vickery S, Price CP, John RI, et al. B-type natriuretic peptide (BNP) and amino-terminal proBNP in patients with CKD: relationship to renal function and left ventricular hypertrophy. *Am J Kidney Dis* 2005;46:610–20.
23. van der Linden N, Cornelis T, Kimenai DM, et al. Origin of cardiac troponin T elevations in chronic kidney disease. *Circulation* 2017;136:1073–5.
24. van Kimmenade RRJ, Januzzi JL, Baggish AL, et al. Amino-terminal pro-brain natriuretic Peptide, renal function, and outcomes in acute heart failure: redefining the cardiorenal interaction? *J Am Coll Cardiol* 2006;48:1621–7.
25. Forfia PR, Watkins SP, Rame JE, Stewart KJ, Shapiro EP. Relationship between B-type natriuretic peptides and pulmonary capillary wedge pressure in the intensive care unit. *J Am Coll Cardiol* 2005;45:1667–71.
26. Burchill L, Velkoska E, Dean RG, et al. Acute kidney injury in the rat causes cardiac remodelling and increases angiotensin-converting enzyme 2 expression. *Exp Physiol* 2008;93:622–30.
27. Kelly KJ. Distant effects of experimental renal ischemia/reperfusion injury. *J Am Soc Nephrol* 2003;14:1549–58.
28. Sumida M, Doi K, Ogasawara E, et al. Regulation of mitochondrial dynamics by dynamin-related protein-1 in acute cardiorenal syndrome. *J Am Soc Nephrol* 2015;26:2378–87.
29. Tokuyama H, Kelly DJ, Zhang Y, Gow RM, Gilbert RE. Macrophage infiltration and cellular proliferation in the non-ischemic kidney and heart following prolonged unilateral renal ischemia. *Nephron Physiol* 2007;106:54–62.
30. Mitaka C, Si MKH, Tulafu M, et al. Effects of atrial natriuretic peptide on inter-organ crosstalk among the kidney, lung, and heart in a rat model of renal ischemia-reperfusion injury. *Intensive Care Med* 2014;2:28.

- 31.** Hulsmans M, Sager HB, Roh JD, et al. Cardiac macrophages promote diastolic dysfunction. *J Exp Med* 2018;215:423–40.
- 32.** Sano H, Hsu DK, Yu L, et al. Human galectin-3 is a novel chemoattractant for monocytes and macrophages. *J Immunol* 2000;165:2156–64.
- 33.** Sharma UC, Pokharel S, van Brakel TJ, et al. Galectin-3 marks activated macrophages in failure-prone hypertrophied hearts and contributes to cardiac dysfunction. *Circulation* 2004;110:3121–8.
- 34.** Henderson NC, Mackinnon AC, Farnworth SL, et al. Galectin-3 expression and secretion links macrophages to the promotion of renal fibrosis. *Am J Pathol* 2008;172:288–98.
- 35.** Hering D, Winklewski PJ. R1 autonomic nervous system in acute kidney injury. *Clin Exp Pharmacol Physiol* 2017;44:162–71.
- 36.** Basile DP, Donohoe DL, Phillips SA, Frisbee JC. Enhanced skeletal muscle arteriolar reactivity to ANG II after recovery from ischemic acute renal failure. *Am J Physiol Regul Integr Comp Physiol* 2005;289:R1770–6.
- 37.** Fernandes Bertocchi AP, Campanhole G, Wang PHM, et al. A role for galectin-3 in renal tissue damage triggered by ischemia and reperfusion injury. *Transpl Int* 2008;21:999–1007.
- 38.** Souza BS de F, Silva DN, Carvalho RH, et al. Association of cardiac galectin-3 expression, myocarditis, and fibrosis in chronic Chagas disease cardiomyopathy. *Am J Pathol* 2017;187:1134–46.
- 39.** Chung AW, Sieling PA, Schenk M, et al. Galectin-3 regulates the innate immune response of human monocytes. *J Infect Dis* 2013;207:947–56.

KEY WORDS fibrosis, heart failure, inflammation, macrophages, renal failure

APPENDIX For an expanded Methods section as well as supplemental figures and tables, please see the online version of this paper.